Pergamon

*Int. J. Engng Sci.* Vol. 35, No. 10/11, pp. 975–986, 1997

Printed in Great Britain
PII: S0020-7225(96)00122-X
0020-7225/97 $17.00 + 0.00

# HYDROMAGNETIC NATURAL CONVECTION FROM AN ISOTHERMAL INCLINED SURFACE ADJACENT TO A THERMALLY STRATIFIED POROUS MEDIUM

ALI J. CHAMKHA

Department of Mechanical and Industrial Engineering, Kuwait University, P.O. Box 5969, Safat, 13060, Kuwait.

**Abstract**—A mathematical model governing free convection boundary-layer flow over an isothermal inclined plate embedded in a thermally stratified porous medium in the presence of a non-uniform transverse magnetic field is developed. The resulting equations account for non-Darcian boundary and inertial effects of the porous medium and allow for variable ambient temperature. In this study, the ambient temperature is assumed to be an increasing function with the distance along the plate and the applied magnetic field is assumed to be a power-law function of the axial or vertical distance. The governing equations are solved subject to appropriate boundary conditions using an implicit finite-difference method. It is found that increases in either of the non-Darcian porous medium inertial parameter or the magnetic field power index, the stratification parameter, or the inclination or full-wedge angle cause reductions in the skin-friction coefficient and the local Nusselt number. Also, as the Hartmann number is increased, both the skin-friction coefficient and the local Nusselt number are increased. © 1997 Elsevier Science Ltd.

## 1. INTRODUCTION

This paper considers laminar, hydromagnetic, natural convection, boundary-layer flow over an isothermal surface embedded in a thermally stratified high-porosity medium. This type of flow is of fundamental importance due to its possible applications in heat exchanger devices, magnetohydrodynamic (MHD) accelerators and generators, filtration, petroleum reservoirs, and others. The open literature is rich with references dealing with forced and natural convection flows over and through different geometries. Some of these references consider non-magnetic flows (see, for instance, Tien and Vafai [1], Chen *et al.* [2], Bejan [3], Takhar and Pop [4], Tewari and Singh [5], Singh and Tewari [6], and Chen and Lin [7]) while others consider magnetic effects in the presence of a porous medium (see, for example, Sparrow and Cess [8], Gupta [9], Riley [10], Kuiken [11], Wilks and Hunt [12], Watanabe and Pop [13], Pop and Watanabe [14] and Chamkha [15]). Both Singh and Tewari [6] and Chen and Lin [7] considered non-Darcy free convection boundary-layer flow along an isothermal vertical plate embedded in a thermally stratified fluid-saturated porous medium including inertia effects (Singh and Tewari [6]) and boundary effects (Chen and Lin [7]). To date, the effects of the presence of a non-uniform transverse magnetic field on the natural convection of an electrically conducting fluid boundary-layer flow in a high porosity and thermally stratified medium have not been considered. The present paper considers this flow situation over an inclined isothermal plate with the applied magnetic field being a power-law function of the distance along the plate. The fluid is assumed incompressible and the flow is assumed laminar. In addition, the magnetic Reynolds number is assumed small so that the induced magnetic field can be neglected.

## 2. GOVERNING EQUATIONS

Consider the problem of steady, laminar, two-dimensional, magnetohydrodynamic free convection flow of an electrically conducting fluid over an isothermal inclined plate embedded in a high porosity medium. The transverse magnetic field which is applied normal to the flow direction is assumed to vary as a power-law function of the distance along the plate and the ambient temperature $T_\infty$ is assumed to vary linearly with the vertical distance. Let the $x$-axis be directed upwards along the plate and the $y$-axis be measured normal to it. The governing equations for this investigation are based on the usual boundary-layer equations modified to include the porous medium effects, the magnetic field effects, and the thermal buoyancy effects. These equations (with the Boussinesq and non-Darcy approximations and neglecting the Hall effects) can be written as (see, Chen and Lin [7], and Chamkha [15])

$$\frac{\partial u}{\partial x} + \frac{\partial v}{\partial y} = 0 \tag{1}$$

$$u\frac{\partial u}{\partial x} + v\frac{\partial u}{\partial y} = \varepsilon^2 g\beta(T - T_\infty(x))\cos(\Omega/2) + \varepsilon\nu\frac{\partial^2 u}{\partial y^2} - \frac{\varepsilon^2\nu}{K}u - \varepsilon^2 C u^2 - \varepsilon^2\frac{\sigma B(x)^2}{\rho}u \tag{2}$$

$$u\frac{\partial T}{\partial x} + v\frac{\partial T}{\partial y} = \alpha_e\frac{\partial^2 T}{\partial y^2} + \frac{\nu}{c_p}\left(\frac{\partial u}{\partial y}\right)^2 + \frac{\sigma B(x)^2}{\rho c_p}u^2. \tag{3}$$

It should be noted that the last two terms of equation (3) represent the viscous and magnetic dissipations, respectively. Similar to Chen and Lin [7], let the ambient temperature take the form

$$T_\infty(x) = T_{\infty,x=0} + sx \tag{4}$$

where $T_{\infty,x=0}$ is the ambient temperature at the leading edge of the plate and $s(>0)$ is a constant which represents the stratification rate or the slope of the ambient temperature profile with $x$. The increasing behavior of the ambient temperature with $x$ indicates that the thermal stratification is stable. It should be mentioned that the temperature of the leading edge of the inclined plate is above that of the surrounding fluid at the same elevation. Also, it must be presumed that the plate has a finite length, otherwise the dominant flow direction will be towards the leading edge of the inclined plate. This occurs when the temperature of the plate falls below that of the surrounding fluid (see, Tewari and Singh [5]).

The physics of the problem suggests the following boundary conditions

$$\begin{aligned} x = 0&: u = 0,\ v = 0,\ T = 0 \\ y = 0&: u = 0,\ v = 0,\ T = T_w \\ y \to \infty&: u \to 0,\ T \to T_\infty(x). \end{aligned} \tag{5}$$

In the present work, it is of interest to understand the effects of allowing the applied magnetic field to vary with the distance along the inclined plate which is the case in a variety of magnetohydrodynamic devices. A reasonable distribution of the magnetic field would be to make $B(x)$ a power-law function of $x$ as follows

$$B(x) = B_0 x^p \tag{6}$$

where $B_0$ is a constant and $p$ is the magnetic field power index.

It is convenient to nondimensionalize the governing equations and boundary conditions. This is accomplished by substituting the following variables:

$$x = L\xi,\ y = L\mathrm{Gr}^{-1/4}\eta,\ u = \frac{\nu}{L}\mathrm{Gr}^{1/2}F,\quad v = \frac{\nu}{L}\mathrm{Gr}^{1/4}G,$$

$$T = (T_w - T_{\infty,x=0})\theta + T_\infty(x),\ \mathrm{Gr} = \frac{g\beta(T_w - T_{\infty,x=0})L^3}{\nu^2} \tag{7}$$

into equations (1)–(6) to yield

$$\frac{\partial F}{\partial \xi} + \frac{\partial G}{\partial \eta} = 0 \tag{8}$$

$$F\frac{\partial F}{\partial \xi} + G\frac{\partial F}{\partial \eta} = \varepsilon^2\theta\cos(\Omega/2) + \varepsilon\frac{\partial^2 F}{\partial \eta^2} - \varepsilon^2\left(\frac{1}{\psi} + M^2\xi^{2p}\right)F - \varepsilon^2\Gamma F^2 \tag{9}$$

$$F\frac{\partial \theta}{\partial \xi} + G\frac{\partial \theta}{\partial \eta} = \frac{1}{\mathrm{Pr}}\frac{\partial^2 \theta}{\partial \eta^2} - SF + \mathrm{Ec}\left(\frac{\partial F}{\partial \eta}\right)^2 + M^2\xi^{2p}\mathrm{Ec}F^2 \tag{10}$$

$$\begin{aligned} &\xi = 0:\ F = 0,\ G = 0,\ \theta = 0\\ &\eta = 0:\ F = 0,\ G = 0,\ \theta = 1 - S\xi\\ &\eta \to \infty:\ F \to 0,\ \theta \to 0 \end{aligned} \tag{11}$$

where

$$\psi = \frac{K\mathrm{Gr}^{1/2}}{L^2},\ \Gamma = CL,\ M^2 = \frac{\sigma B_0^2 L^2}{\rho\nu\mathrm{Gr}^{1/2}},\ \mathrm{Pr} = \frac{\nu}{\alpha_e},$$

$$\mathrm{Ec} = \frac{\nu^2\mathrm{Gr}}{c_p L^2(T_w - T_{\infty,x=0})},\ S = \frac{L}{(T_w - T_{\infty,x=0})}\frac{\mathrm{d}T_\infty(x)}{\mathrm{d}x}. \tag{12}$$

Important physical parameters for this type of flow situation are the skin-friction coefficient and the local Nusselt number. These can be shown to take the following dimensionless forms:

$$C_\mathrm{f} = -\mathrm{Gr}^{3/4}\frac{\partial F}{\partial \eta}\bigg|_{\eta=0},\ \mathrm{Nu}_x = -\mathrm{Gr}^{1/4}\frac{\xi}{1 - S\xi}\frac{\partial \theta}{\partial \eta}\bigg|_{\eta=0}. \tag{13}$$

## 3. RESULTS AND DISCUSSION

Equations (8)–(10) are coupled nonlinear partial differential equations which possess no similarity or closed-form solutions. Therefore, a numerical solution of the problem under consideration is needed. However, if some of the terms in the governing equations are neglected and some idealized assumptions are made, a closed-form solution is possible. This solution will be helpful in validating the numerical results.

A limiting special case of the problem considered in the paper is that of natural convection flow over an infinitely long inclined porous plate in the presence of a uniform transverse magnetic field directed normal to the flow direction. Assuming that the plate temperature is uniform and that the ambient temperature is nonstratified and if other idealized assumptions are made, the governing equations for this special case can be solved analytically. This analytical

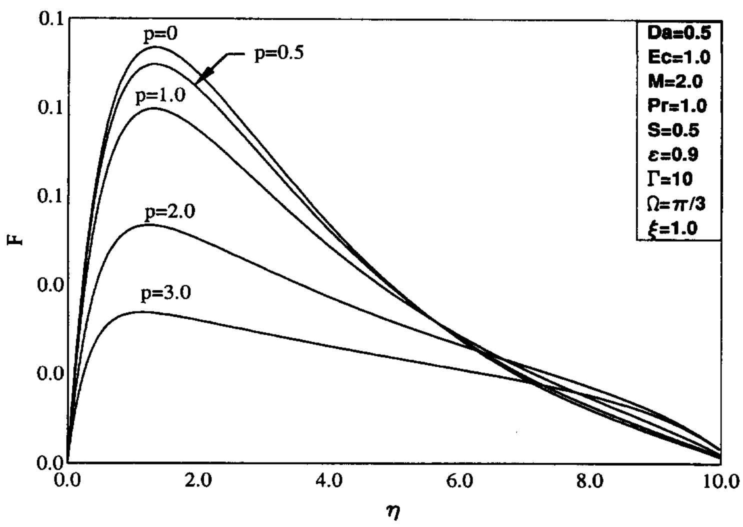


Fig. 1.

solution provides a check on the correctness of the fully numerical solutions of the general equations given by equations (8)–(11). The governing equations and conditions for this special case can be obtained from equations (8)–(11) by formally setting $\dfrac{\partial(\ )}{\partial\xi}=0$, $p=0$ and $S=0$. These can be written as

$$G'=0 \tag{14}$$

$$\varepsilon F' - GF' - \varepsilon^2\left(\frac{1}{\psi}+M^2\right)F - \varepsilon^2\Gamma F^2 + \varepsilon^2\theta\cos(\Omega/2)=0 \tag{15}$$

$$\frac{1}{\mathrm{Pr}}\theta'' - G\theta' + \mathrm{Ec}F'^2 + M^2\mathrm{Ec}F^2=0 \tag{16}$$

$$\eta=0\colon F=0,\ G=-G_0,\ \theta=1,\ \eta\to\infty\colon F\to 0,\ \theta\to 0 \tag{17}$$

where a prime denotes ordinary differentiation with respect to $\eta$ and $G_0$ ($>0$) is a prescribed suction velocity.

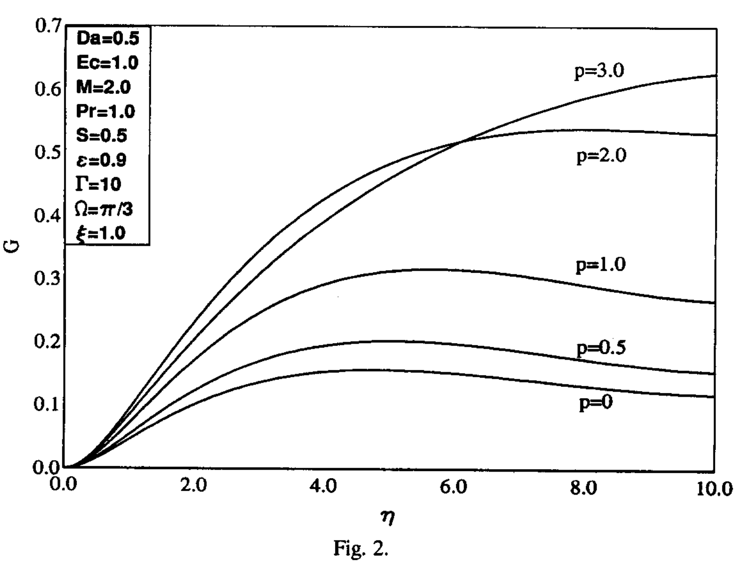


Fig. 2.

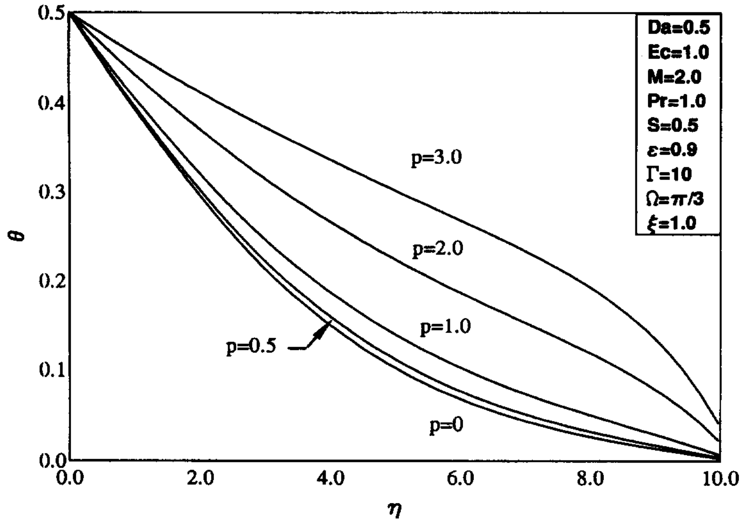


Fig. 3.

Neglecting the porous medium inertial effects and the viscous and magnetic dissipation terms in equations (15) and (16), the following closed-form solutions result

$$\theta = \exp(-G_0 \mathrm{Pr}\eta) \tag{18}$$

$$F = A(\exp(-G_0\mathrm{Pr}\eta) - \exp(-\lambda\eta)) \tag{19}$$

where

$$A = \frac{\varepsilon^2\cos(\Omega/2)}{G_0^2\mathrm{Pr}(1-\varepsilon\mathrm{Pr}) + \varepsilon^2\left(\dfrac{1}{\psi} + M^2\right)},\ \lambda = \frac{G_0 + \left(G_0^2 + 4\varepsilon^3\left(\dfrac{1}{\psi} + M^2\right)\right)^{1/2}}{2\varepsilon}. \tag{20}$$

The skin-friction coefficient and the Nusselt number can be shown to be

$$C_f = \mathrm{Gr}^{3/4}A(G_0\mathrm{Pr} - \lambda),\ \mathrm{Nu} = \mathrm{Gr}^{1/4}G_0\mathrm{Pr}. \tag{21}$$

The full equations (8)–(10) are solved numerically subject to equation (11) using an implicit, tri-diagonal, variable step size finite-difference methodology similar to that discussed by

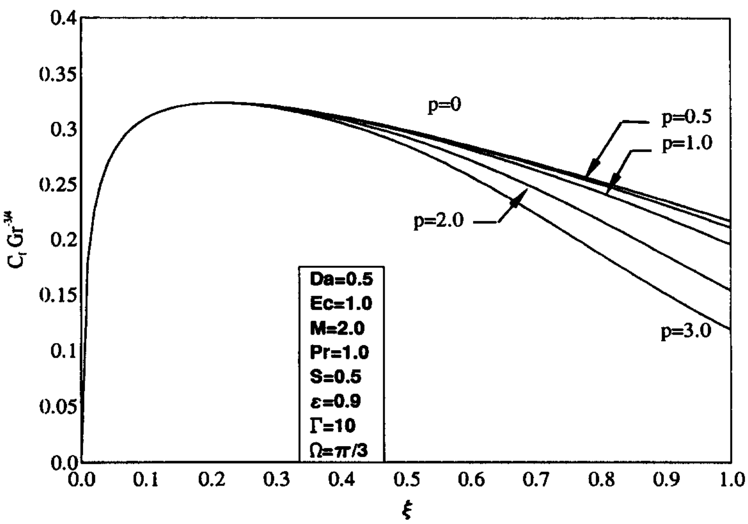


Fig. 4.

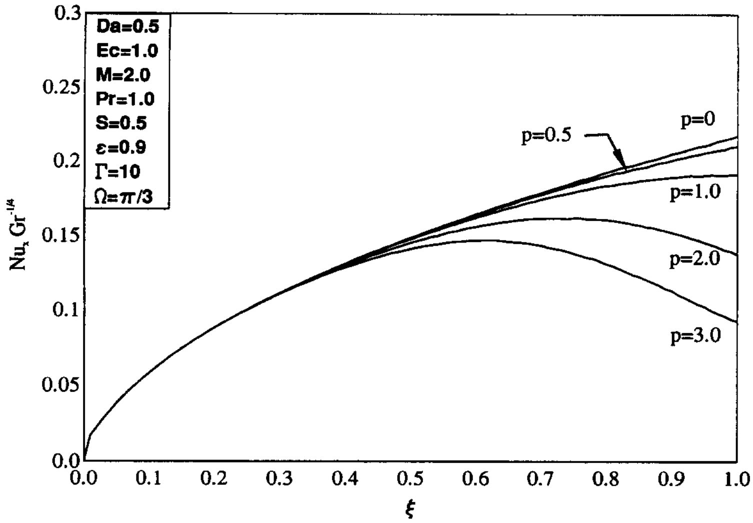


Fig. 5.

Blottner [16] and Patankar [17]. The computational domain is divided into 196 nodes in the $\eta$ direction and 301 nodes in the $\xi$ direction. Variable step sizes in both directions are used. The initial step sizes and the growth factors in the $\eta$ and $\xi$ directions are 0.001, 1.03, and 0.01, 1.01, respectively. All first-order derivatives with respect to $\xi$ are replaced by two-point backward difference formulas. Equations (9) and (10) are discretized using three-point central difference quotients while $\eta$ differencing of equation (8) is accomplished using the trapezoidal rule. The problem is solved as an initial-value problem with $\xi$ playing the role of time. At each line of constant $\xi$, linear tri-diagonal matrix of linear algebraic equations are solved using the Thomas' algorithms (see Blottner [16],) with iteration being used to deal with the nonlinearities of the governing equations. A convergence criterion based on the difference of the current and the previous iterations is set to $10^{-5}$. It should be mentioned that the choice of the initial step sizes and the growth factors in the $\xi$ and $\eta$ directions was arrived at after performing many numerical experimentations to ensure grid independence. In fact, when $\Delta\eta_1$ was set to 0.01 instead of 0.001, an error of about 3% resulted. In addition, setting $\Delta\xi_1$ to 0.1 instead of 0.01 yielded an error of about 4%. In what follows, Figs 1–15 represent purely numerical results

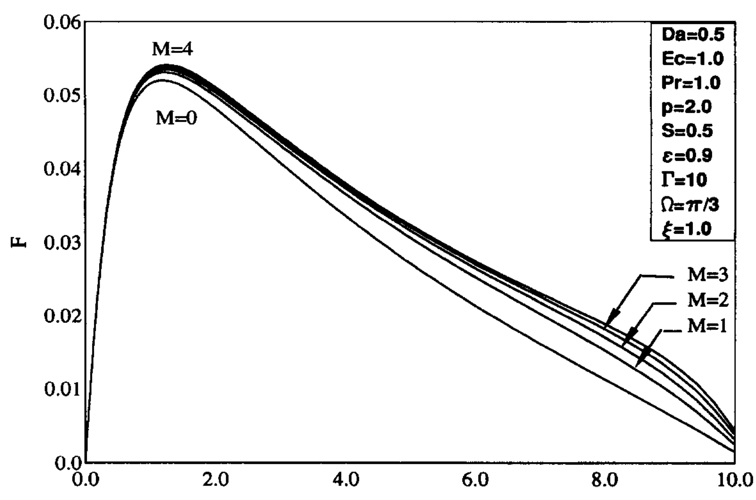


Fig. 6.

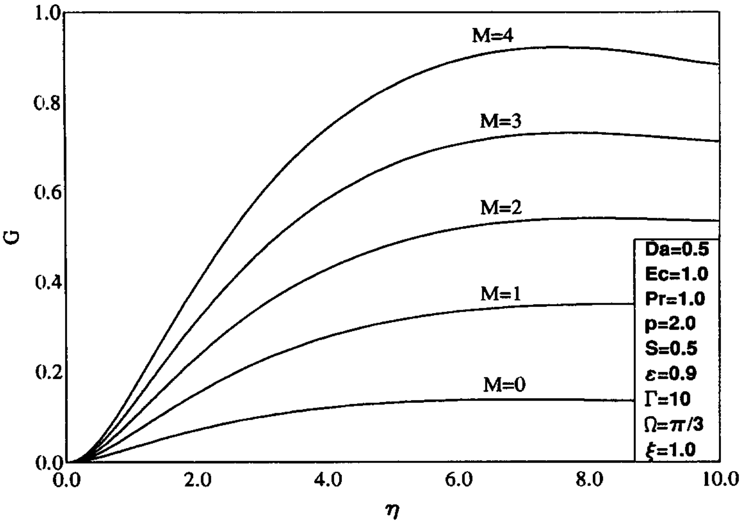


Fig. 7.

which illustrate the effect of various physical parameters on the flow and heat transfer aspects of the present problem.

Figures 1–3 show typical tangential velocity ($F$), normal velocity ($G$), and temperature ($\theta$) profiles at $\xi=1$ and an inclination angle $\Omega=\pi/3$ for various values of the power index $p$ of the magnetic field distribution, respectively. In general, application of a transverse magnetic field normal to the flow direction has a tendency to induce a flow-resistive force in the $x$-direction. This force tends to slow down the motion of the fluid upwards along the inclined plate. Increasing the value of $p$ has the direct effect of increasing the Hartmann magnetic strength. This produces a decrease in the tangential velocity, a spread or increase in the normal velocity, and an increase in the temperature of the fluid as clearly shown in Figs 1–3.

Figures 4 and 5 illustrate the influence of the power index $p$ on the skin-friction coefficient $C_f$ and the local Nusselt number $Nu_x$ along the inclined plate, respectively. At the leading edge of the inclined plate ($\xi=0$), the fluid tangential velocity and temperature are assumed equal to zero. This causes both of $C_f$ and $Nu_x$ to vanish there. As the flow is induced due to thermal buoyancy effects along the plate, the tangential velocity and temperature gradients at the wall

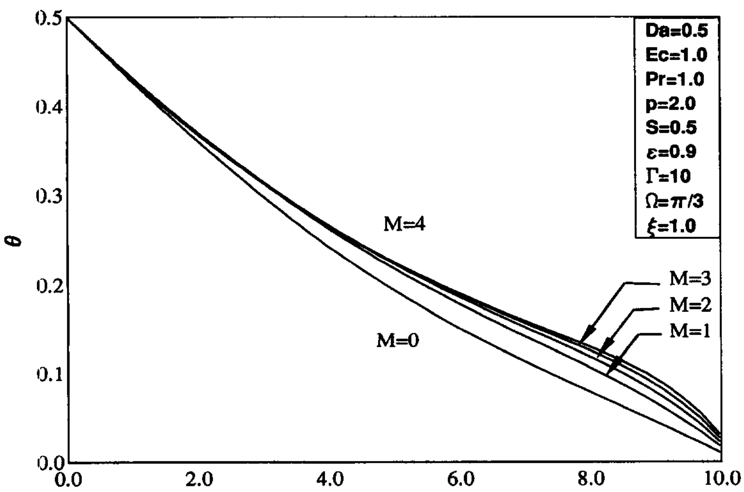


Fig. 8.

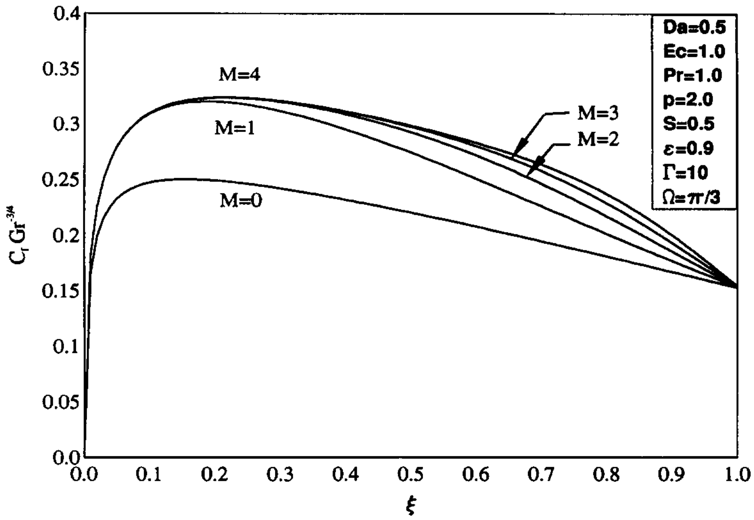


Fig. 9.

increase resulting in increases in both of $C_f$ and $Nu_x$ as $\xi$ increases. These increases in $C_f$ and $Nu_x$ tend to reach maxima at positions around $\xi = 0.15$ for $C_f$ and $\xi > 0.7$ (depending on the values of $p$) for $Nu_x$. In addition, the reductions and increases in the values of $F$ and $\theta$, respectively, as $p$ increases cause reductions in both of the wall tangential velocity and temperature gradients. Consequently, both of $C_f$ and $Nu_x$ decrease as $p$ increases as clearly depicted in Figs 3 and 4. It is also seen from these figures that the effect of $p$ on $C_f$ and $Nu_x$ is limited to the region $\xi > 0.5$ far downstream from the inclined plate's leading edge.

Figures 6–10 present typical profiles for $F$, $G$, and $\theta$ at $\xi = 1$ and the development of $C_f$ and $Nu_x$ along the inclined surface for various values of the Hartmann number $M$, respectively. It is well known that the application of a uniform magnetic field normal to the flow direction causes reductions in the velocity of the fluid (see Chamkha [15]). This seems not to be the case for the present problem where the applied magnetic field is assumed to vary with the distance along the plate. In fact, as the Hartmann number increases, all of the fluid hydrodynamic and thermal characteristics increase. This interesting phenomenon is demonstrated by the increases in $F$, $G$, $\theta$, $C_f$, and $Nu_x$ as $M$ increases as shown in Figs 6–10, respectively. A very important result

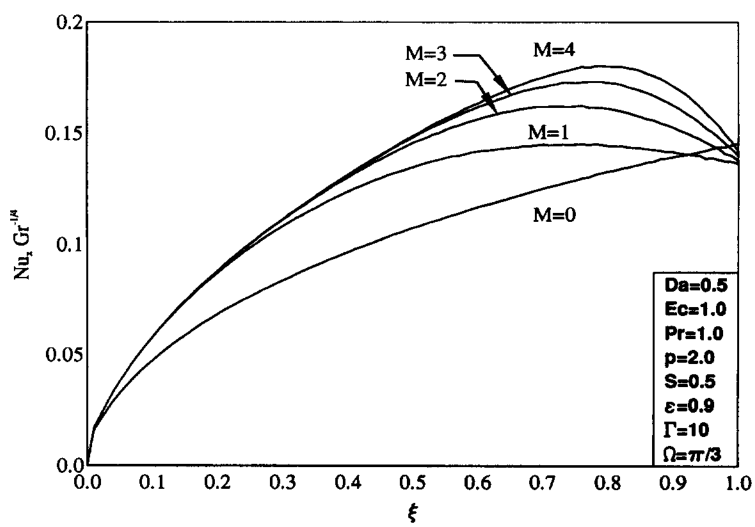


Fig. 10.

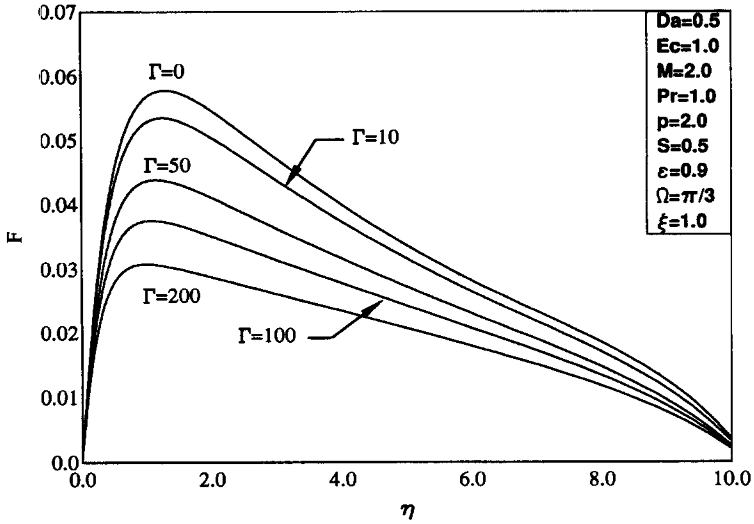


Fig. 11.

therein is that the local Nusselt number along the inclined surface is augmented by the application of a non-uniform magnetic field.

Figures 11–15 present the same variables presented in Figs 6–10, respectively, for different values of the non-Darcian porous medium inertia coefficient Γ. The presence of a porous medium in the system under consideration in the present problem represents an obstacle or resistance to the flow. This resistance is amplified by increasing Γ and has the effect of reducing the fluid tangential and normal velocity components and increasing the fluid temperature. This, in turn, results in decreasing both the skin-friction coefficient and the local Nusselt number for the reasons mentioned in the previous paragraph. This is clearly depicted in Figs 11–15.

It is worth mentioning that it was found from results not presented here, for brevity and because they are known from the open literature, that increasing either of the full-wedge angle Ω or the stratification parameter $S$ caused both the skin-friction coefficient $C_f$ and the local Nusselt number $Nu_x$ to decrease. It was observed that while the effect of increasing $S$ on $C_f$ is felt in the region very close to the leading edge of the inclined plate ($\xi = 0.05$) and becomes

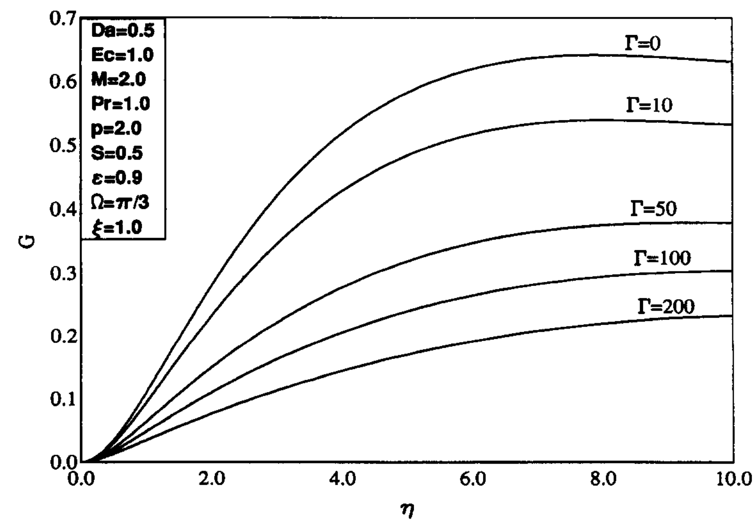


Fig. 12.

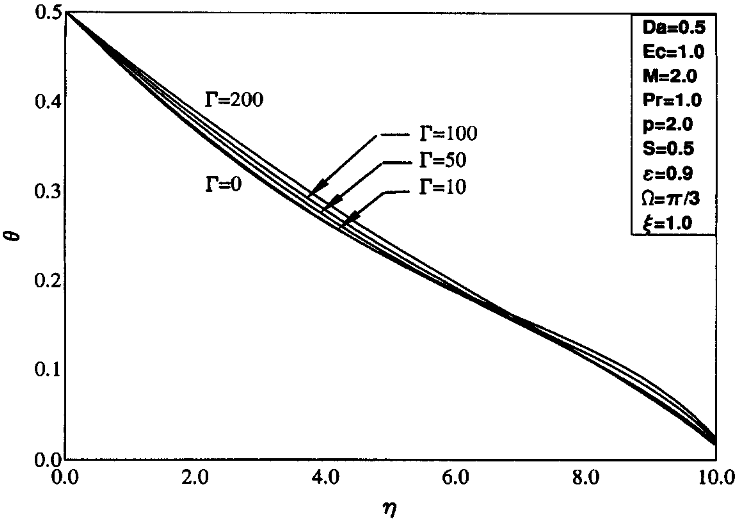


Fig. 13.

more pronounced further downstream as $\xi$ increases, its influence on $Nu_x$ is limited to the region $\xi > 0.7$. These behaviors are consistent with results published in the open literature (see, Gebhart *et al.* [18]).

It should be noted that all the numerical results reported herein for the special case of $M = 0$ (no magnetic field) and $\Omega = 0$ (vertical plate) and in the absence of viscous dissipation are in excellent agreement with the results reported by Chen and Lin [7]. Also, comparisons with the previously published work of Chamkha [15] for the case where $\Omega = 0$ and constant or uniform applied magnetic field were made and excellent agreement with results was found. In addition, favorable comparisons with the closed-form solutions developed earlier in this paper were obtained. These several comparisons provided separate checks on the validity and correctness of the numerical solutions. It should be noted, however, that the physical phenomena and the interesting features predicted in the present work can only be physically validated by comparing the present results with experimental data. These data appear to be lacking at present and an experimental effort is being planned for this purpose.

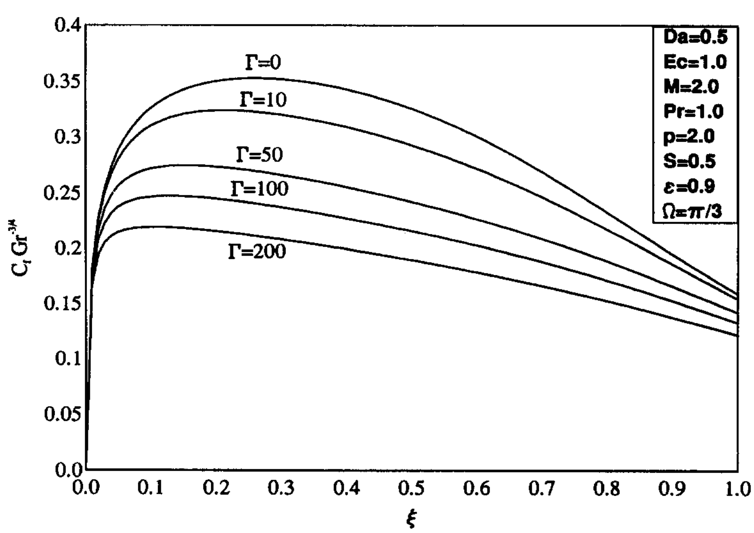


Fig. 14.

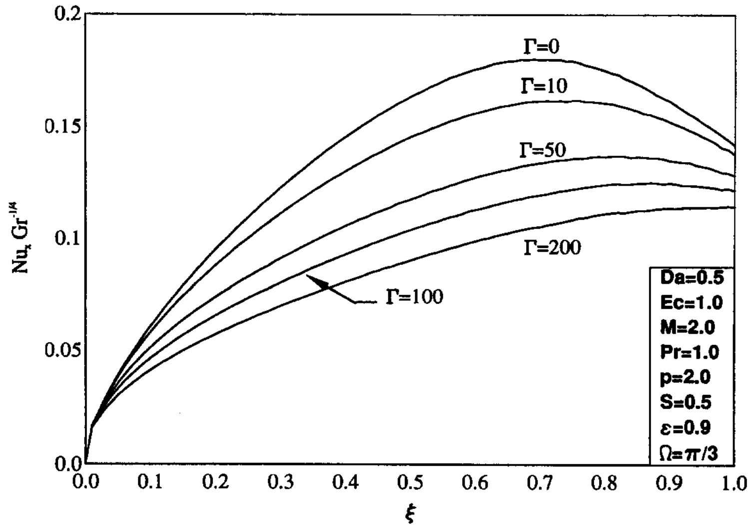


Fig. 15.

## 4. CONCLUSION

The problem of free convection boundary-layer flow along an inclined plate embedded in a thermally stratified porous medium in the presence of a variable magnetic field was solved numerically by an implicit and iterative finite-difference method. The plate is assumed isothermal and the applied transverse magnetic field is assumed to vary with the distance along the plate in the form of a power-law function. The mathematical model representing the problem included non-Darcian boundary and inertial effects of the porous medium as well as viscous and magnetic dissipations. Numerical results illustrating interesting predicted phenomena were presented graphically. It was found that the presence of the non-uniform applied transverse magnetic field caused both the skin-friction coefficient and the local Nusselt number along the plate length to increase while the presence of the porous medium inertial effects caused these properties to decrease. In addition, increases in either of the magnetic field power index, stratification parameter, or the full-wedge or inclination angle caused reductions in both of the skin-friction coefficient and the local Nusselt number. Comparisons of the numerical results with previously published work and closed-form solutions for a simplified problem were made and found to be in excellent agreement. No comparisons with experimental data were made due to the absence of such data at present. It is hoped that the present results be used for understanding more complex problems dealing with magnetohydrodynamic free convection in porous media.

## REFERENCES

1. Tien, C. L. and Vafai, K., *Adv. Appl. Mech.*, 1990, **27**, 225.
2. Chen, C. K., Hung, C. I. and Horng, H. C., *ASME J. Energy Res. Tech.*, 1987, **109**, 112.
3. Bejan, A., *Convection Heat Transfer*, Wiley, New York, 1984, pp. 367–371.
4. Takhar, H. S. and Pop, I., *Mech. Res. Commun.*, 1987, **14**, 81.
5. Tewari, K. and Singh, P., *Int. J. Engng. Sci.*, 1992, **30**, 1003.
6. Singh, P. and Tewari, K., *Int. J. Engng. Sci.*, 1993, **31**, 1233.
7. Chen, C. and Lin, C., *Int. J. Engng. Sci.*, 1995, **33**, 131.
8. Sparrow, E. M. and Cess, R. D., *Int. J. Heat Mass Transfer*, 1961, **3**, 267.
9. Gupta, A. S., *J. Appl. Math. Phys. (ZAMP)*, 1963, **13**, 324.
10. Riley, N. J., *Fluid Mech.*, 1964, **18**, 577.
11. Kuiken, H. K., *J. Engng. Math.*, 1971, **5**, 51.
12. Wilks, G. and Hunt, R., *J. Appl. Math. Phys. (ZAMP)*, 1984, **35**, 34.
13. Watanabe, T. and Pop, I., *Int. Comm. Heat Mass Transfer*, 1993, **20**, 871.
14. Pop, I. and Watanabe, T., *Int. J. Engng. Sci.*, 1994, **32**,, 1903.
15. Chamkha, A.J., *Fluid/Particle Separation Journal*, 1996, **9**, 195.

16. Blottner, F. G., *AIAA Journal*, 1970, **8**, 193.
17. Patankar, S.V., *Numerical Heat Transfer and Fluid Flow*, McGraw–Hill, New York, 1980.
18. Gebhart, B., Jaluria, Y., Mahajan, R.L. and Sammakia, B., *Buoyancy-Induced Flows and Transport*, Hemisphere Publishing Corporation, New York, 1988, pp. 170–175.

*(Received 13 June 1996; accepted 4 October 1996)*

## NOMENCLATURE

| | |
|---|---|
| $B(x)$ | variable magnetic field |
| $B_0$ | magnetic induction coefficient (a constant) |
| $c_p$ | fluid specific heat at constant pressure |
| $C$ | dimensional porous medium inertia coefficient |
| $C_f$ | skin-friction coefficient |
| Ec | Eckert number |
| $F$ | dimensionless fluid tangential velocity |
| $g$ | gravitational acceleration |
| $G$ | dimensionless fluid normal velocity |
| $G_0$ | suction velocity |
| Gr | Grashof number |
| $K$ | permeability of porous medium |
| $L$ | characteristic length |
| $M$ | Hartmann number |
| Nu | Nusselt number |
| $Nu_x$ | local Nusselt number |
| $p$ | magnetic field power index |
| Pr | effective Prandtl number |
| $s$ | dimensional stratification parameter |
| $S$ | dimensionless stratification coefficient |
| $T$ | dimensional fluid temperature |
| $u$ | dimensional $x$-component of fluid velocity |
| $v$ | dimensional $y$-component of fluid velocity |
| $x$ | dimensional distance along the plate |
| $y$ | dimensional horizontal distance normal to $x$ |

*Greek symbols*

| | |
|---|---|
| $\alpha_e$ | effective thermal diffusivity of porous medium |
| $\eta$ | dimensionless normal distance |
| $\beta$ | volumetric thermal expansion coefficient |
| $\Omega$ | inclination or full-wedge angle |
| $\epsilon$ | porosity of medium |
| $\psi$ | Darcy number |
| $\nu$ | fluid kinematic viscosity |
| $\rho$ | fluid density |
| $\sigma$ | fluid electrical conductivity |
| $\theta$ | dimensionless fluid temperature |
| $\xi$ | dimensionless axial distance |

*Subscripts*

| | |
|---|---|
| $\infty$ | ambient conditions |
| w | wall |